# Four-Stranded Aggregates of Oligodeoxyguanylates Forming Lyotropic Liquid Crystals: A Study by Circular Dichroism, Optical Microscopy, and X-ray Diffraction

**Stefania Bonazzi,[†,‡] Massimo Capobianco,[‡] Monica Miranda De Morais,[§] Anna Garbesi,*[,‡] Giovanni Gottarelli,*[,†] Paolo Mariani,*[,§] Maria Grazia Ponzi Bossi,[§] Gian Piero Spada,*[,†] and Luisa Tondelli[‡]**

*Contribution from the Dipartimento di Chimica Organica "A. Mangini", Università di Bologna, via S. Donato 15, I-40127 Bologna, Italy, I.Co.C.E.A.-CNR, via della Chimica 8, I-40064 Ozzano Emilia (BO), Italy, and Istituto di Fisica Medica, Università di Ancona, Monte d'Ago, I-60131 Ancona, Italy.* *Received December 27, 1990. Revised Manuscript Received March 25, 1991*

**Abstract:** The guanosine derivatives d(pG), d(GpG), d(GpGpG), d(GpGpGpG), and d(GpGpGpGpGpG), dissolved in water, give rise to cholesteric and hexagonal mesophases. These phases were investigated by X-ray diffraction, optical microscopy, and circular dichroism. The building block of these phases is a chiral rod-shaped aggregate composed of a stacked array of Hoogsteen-bonded guanosine tetramers. The ability of the different derivatives to originate the liquid-crystalline phases is discussed. Circular dichroism measurements show that the chirality of the rod-shaped aggregates is not the same for the five derivatives as is reflected also by the different handedness and pitches of the relative cholesteric phases. This seems to depend on the *ratio* between covalent and noncovalent bonds holding together the oligodeoxyguanylates in the chiral rod-shaped aggregates.

It is known that concentrated solutions of DNA,[1] polyribonucleotides,[2] and self-complementary oligodeoxynucleotides[3] can spontaneously organize themselves to form lyomesophases. In recent papers we reported that the non-self-complementary dinucleoside phosphate d(GpG) (**G2**) in aqueous solutions gives rise to cholesteric and hexagonal mesophases,[4] the structures of which were further investigated by X-ray diffraction.[5] Here we report that the nucleotide 2'-deoxyguanosine 5'-monophosphate d(pG) (**G1**), the "trimer" d(GpGpG) (**G3**), the "tetramer" d(GpGpGpG) (**G4**), and the "hexamer" d(GpGpGpGpGpG) (**G6**) also form cholesteric and hexagonal phases.

While the overall structure of the columnar aggregates, which are the building blocks of the mesophases, are similar to each other and to that of **G2** previously reported[4,5] [i.e., each chiral rod is similar to a four-stranded helix and is composed of a stacked array of planar tetrameters formed by Hoogsteen-bonded guanosine moieties (see Figure 1)], differences were observed in the handedness of the cholesteric phases and in the concentration values at which phase transitions occur.

This study describes the supermolecular chemistry of molecules of biological[6] and prebiotic[7] significance. Their association eventually leads to the formation of liquid-crystalline phases which are studied by X-ray diffraction. In this way we obtain information on guanine aggregates in a fluid aqueous phase, similar to the conditions observed in biological systems. Our data, together with those obtained on other model systems,[8] might be of use in view of the recent suggestion[6] that the formation of guanine tetrads mediates the pairing in a parallel fashion of the four homologous chromatides during the meiosis and the dimerization of the telomeric ends of chromosomes.

## Results

**Optical Microscopy.** Preliminary observations were carried out on samples with concentration gradient obtained by peripheral evaporation or by allowing water to penetrate into the neat sample. For each of the four derivatives **G1**, **G3**, **G4**, and **G6**, these observations show the existence of at least two phases[9] which have been identified from the textures as cholesteric and hexagonal at higher and lower water content, respectively.[4,5] Successively the textures were studied as a function of the concentration (here expressed in weight of solute percent weight of solution), giving the following phase sequence

**G1**: I 30% N* 40% H

**G2**: I 2.5% N* 18% H (from ref 5)

**G3**: I 8% N* 25% H

**G4**: I 13% N* ≈35% H

**G6**: I 18-20% N* 35% H

**Chart I**

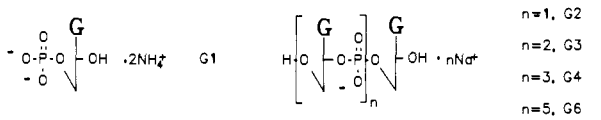


**Chart II**

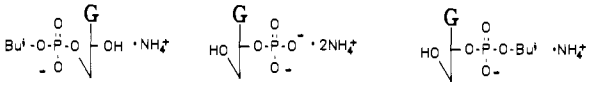


[†] Università di Bologna.
[‡] I.Co.C.E.A.-CNR, Bologna.
[§] Università di Ancona.

(1) Robinson, C. *Tetrahedron* **1961**, *13*, 219. Brandes. R.; Kearns, D. R. *Biochemistry 1986*, *25*, 5890. Yevdokimov, Y. M.; Skuridin, S. G.; Salyanov, V. I. *Liq. Cryst.* **1988**, *3*, 1443-59. Livolant, F.; Levelut, A. M.; Doucet, J.; Benoit, J. P. *Nature* **1989**, *339*, 724-6. Van Winkle, D. H.; Davidson, M. W.; Chen, W.-X.; Rill, R. L. *Macromolecules* **1990**, *23*, 4140-8. See, also: references cited therein.

(2) Iizuka, E. *Polymer J.* **1983**, *15*, 525-35. Iizuka, E. *Adv. Biophys.* **1988**, *24*, 1-56. Tondorf, I.; Lichtenberger. O.; Hoffmann, S. *Z. Chem.* **1990**, *30*, 171. See, also: references cited therein.

(3) Alam, T. M.; Drobny, G. *Biochemistry* **1990**, *29*, 3421-30.

(4) Spada, G. P.; Carcuro, A.: Colonna, F. P.: Garbesi, A.; Gottarelli, G. *Liq. Cryst.* **1988**, *3*, 651-4.

(5) Mariani, P.; Mazabard, C.; Garbesi, A.; Spada, G. P. *J. Am. Chem. Soc.* **1989**, *111*, 6369-73.

(6) Sen, D.; Gilbert, W. *Nature (London)* **1988**, *334*, 364-6; **1990**, *344*, 410. Sundquist, W. I.; Klug, A. *Nature (London)* **1989**, *342*, 825-9. See, also: references therein.

(7) Detellier. C.; Laszlo, P. *Helv. Chim. Acta* **1979**, *62*, 1559-65. Pinnavaia. T. J.; Marshall, C. L.; Mettler, C. M.; Fisk, C. L.; Miles, H. T.; Becker, E. D. *J. Am. Chem. Soc.* **1978**, *100*, 3625-7. Detellier, C.; Laslo, P. *J. Am. Chem. Soc.* **1980**, *102*, 1135-41.

(8) Jin, R.; Breslauer, K. J.: Jones. R. A.; Gaffney, B. L. *Science* **1990**, *250*, 543-6.

0002-7863/91/1513-5809$02.50/0 

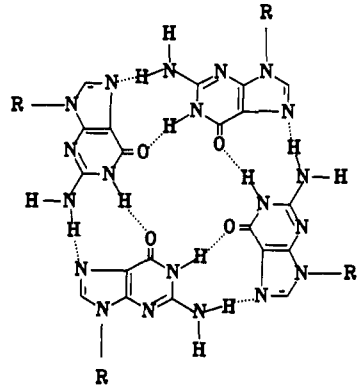

Figure 1. A tetramer of Hoogsteen-bonded guanine residues.

where I, N*, and H denote isotropic, cholesteric, and hexagonal phases, respectively. The critical concentration ($c_0$) at which the cholesteric phase appears increases in the order **G2**, **G3**, **G4**, **G6**, and **G1**.[11] As the behavior of **G1** seems to be outside the trend exhibited by the other derivatives, we synthetized the isobutyl ester of **G1**, **1**, in order to test the importance of lipophilicity on its ability to form liquid–crystalline phases. To our surprise, this derivative does not show the formation of any liquid–crystalline phase. In addition, we extended our investigation to 2′-deoxyguanosine 3′-monophosphate d(Gp), **2**. This compound gives at least two LC (liquid crystalline) phases, the former of which appears at a concentration of ca. 5%.[12] Also its isobutyl ester **3** exhibits two LC phases starting from a concentration of ca. 25%. It seems evident that for the monomeric derivatives, the hydrophilic/hydrophobic balance is certainly not the determining factor; instead the location of the phosphate groups and also the sterochemical constraints imposed by the presence of the isobutyl group play a major role on the ability to form LC phases.

For the homogeneous series **G2**, **G3**, **G4**, and **G6**, which does not possess a free phosphate end group, the critical concentration at which the cholesteric phase appears seems to follow a definite pattern related to the ratio of negative charge/guanine units. This ratio increases in the sequence **G2**, **G3**, **G4**, and **G6** and is indicative of both the electrostatic interaction and the hydrophilic/hydrophobic balance. The smaller this ratio, the easier the formation of the LC phases.

The cholesteric phases can easily be aligned with a magnetic field. When the field is parallel to the cell walls, fingerprint textures are obtained from which the pitch of the cholesteric helix can readily be established;[4,5] the helix is not unwound by the field. When the field is perpendicular to the cell walls, a planar texture is obtained; this configuration will be used for circular dichroism (CD) studies as in this case the helix axis is perpendicular to the cell walls and in the same direction as the circularly polarized light impinging on the sample. As for **G2**, this behavior indicates that the objects which compose the phases have negative diamagnetic anisotropy (type II cholesteric).[13] The pitches of cholesteric

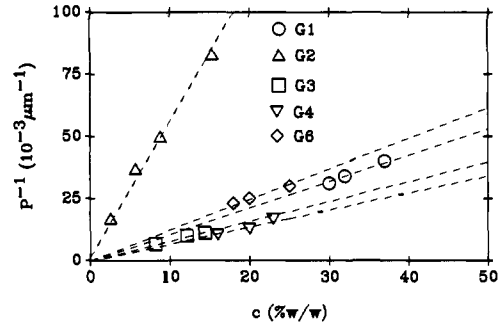


Figure 2. Plots of the inverse pitch vs concentration for the cholesteric solutions of **G1**, **G2** (from ref 4), **G3**, **G4** and **G6**.

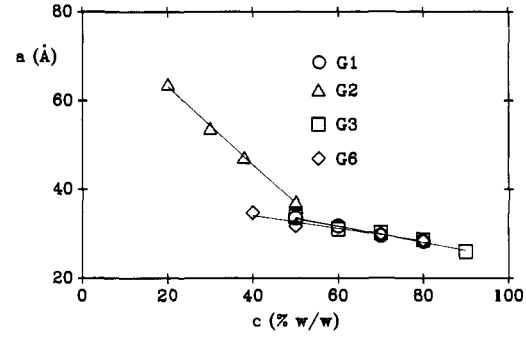


Figure 3. Variations of the dimension of the unit cell ($a$) in the hexagonal phase at 25 °C as a function of guanosine derivative concentration. Data for **G2** are taken from ref 5.

solutions of compounds **G1**, **G3**, **G4**, and **G6** show an inverse dependence on the concentration as reported for **G2**[4] (see Figure 2).

**X-ray Diffraction.** The X-ray diffraction results on the **G1**, **G3**, and **G6** lyomesophases are consistent with the phase sequence obtained by optical microscopy, confirming the presence of three distinct structural organizations as a function of water content: cholesteric, hexagonal, and crystal phases were in fact identified going from the more hydrated to the dry samples. In particular, X-ray diffraction experiments were performed as a function of the water content of the solutions of the three **G1**, **G3**, and **G6** derivatives: in Table I is reported the list of the investigated samples with some crystallographic information. Without going into detail for the crystalline structures, the X-ray diffraction patterns obtained in the different phases appeared to be equivalent in the three derivatives and also in perfect agreement with the ones reported in ref 5 for the case of the **G2**/water system. In the low angle X-ray diffraction region ($S < (10\ \text{Å})^{-1}$),[14] the profiles are typically characterized by a diffused broad peak (the position of this band seems to be strongly dependent on the sample water content)[15] when the samples observed with the microscope show the cholesteric texture, while, in correspondence to the phase identified as hexagonal by optical microscopy, the pattern presents a very intense and sharp reflection together with two or three other very weak peaks, the spacing ratios of which clearly indicate the two-dimensional hexagonal packing.[16] The high angle region ($S > (10\ \text{Å})^{-1}$) is characterized, in both hexagonal and cholesteric phases, by a sharp peak at about $S = (3.3\ \text{Å})^{-1}$. This peak is not

(9) In contrast to the other oligoguanylates investigated, **G1** lyomesophases are not easily obtained with the sodium salt of the nucleotide. Liquid–crystalline phases are better obtained with ammonium as a counterion. The effect of the ion specificity in stabilizing aggregation of guanosine monophosphates has already been reported,[7,10] and our findings agree with these data.

(10) Walmsley, J. A.; Barr, R. G.; Bouhoutsos-Brown, E.; Pinnavaia, T. J. *J. Phys. Chem.* **1984**, *88*, 2599–605. Barr, R. G.; Pinnavaia, T. J. *J. Phys. Chem.* **1986**, *90*, 328–34. Fisk, C. L.; Becker, E. D.; Miles, H. T.; Pinnavaia. T. J. *J. Am. Chem. Soc.* **1982**, *104*, 3307–14. See, also: references therein.

(11) The phosphodiester groups of oligonucleotides in water solution are fully ionized, the $pK_a$ of the P–OH function being approximately equal to 1 (see for example: Cantor, C. R.; Schimmel, P. R. *Biophysical Chemistry*; Freeman: San Francisco, 1980). Also the end phosphate group present in **G1** is not protonated in neutral condition[7,10] and hence maintains its dianionic form.

(12) Microscopic observations of the low concentration phase seem to indicate, also in this case, a cholesteric structure. However we could not obtain a fingerprint texture even after a long permanence of the sample in a magnetic field; also no homogeneous planar texture could be obtained. The phases formed by this compound therefore require further investigation.

(13) Radley, K.; Saupe, A. *Mol. Phys.* **1978**, *42*, 493. Yu, L. J.; Saupe, A. *J. Am. Chem. Soc.* **1980**, *102*, 4879. Boden. N.; Radley, K.; Holmes, M. C. *Mol. Phys.* **1981**, *42*, 493. Alcantara, M. R.; De Melo. M. V. M. C.; Paoli, V. R.; Vanin, J. A. *Mol. Cryst. Liq. Cryst.* **1983**, *95*, 299. Melnik, J.; Saupe, A. *Mol. Cryst. Liq. Cryst.* **1987**, *145*. 95–110.

(14) $S$ (expressed in $\text{Å}^{-1}$) is defined as 2 sin $\theta/\lambda$, $2\theta$ being the X-ray scattering angle and $\lambda$ the X-ray wavelength.

(15) Mariani, P.; Micheletto. R.; Spada, G. P.; Amaral, L.; Itri. R. Work in progress.

(16) By using the convention usually adopted in lipid crystallography (see refs 17 and 18), the reflections permitted in the case of a bidimensional hexagonal symmetry (space group $p6$) are given by $S(h,k) = (1/a)(4/3)^{1/2}(h^2 + k^2 - hk)^{1/2}$, where $a$ is the unit cell dimension and $h,k$ are the Miller indexes of the reflection.

**Table I.** Experimental X-ray Diffraction Data[a]

Derivative: **G1**

| $c$, % w/w | 30 | 40 | 50 | 60 | 70 | 80 |
|---|---|---|---|---|---|---|
| phase | N* | N* | H | H | H | H |
| $a$, Å | | | 33.62 | 31.75 | 29.55 | 28.39 |
| low angle | | | | $S$, $10^{-3}$ Å$^{-1}$ | | |
| | | cal obs | cal obs | cal obs | cal obs | cal obs |
| $(h^2 + k^2 - hk)$ | | | | | | |
| 1 | | 34.3 34.3 | 36.4 36.3 | 39.1 39.1 | 40.7 | 40.6 |
| 3 | | 59.5 59.6 | 63.0 63.0 | 67.7 67.5 | 70.4 | 70.7 |
| 4 | | 68.7 68.8 | 72.7 73.0 | 78.2 78.0 | 81.3 | 81.2 |
| 7 | | 90.9 90.6 | 96.2 | 103.4 103.7 | 107.6 | |
| high angle | | | | $S \pm 0.02$, Å$^{-1}$ | | |
| | $(3.39)^{-1}$ | $(3.38)^{-1}$ | $(3.38)^{-1}$ | $(3.39)^{-1}$ | $(3.41)^{-1}$ | $(3.37)^{-1}$ |

Derivative: **G3**

| $c$, % w/w | 20 | 50 | 60 | 70 | 80 | 90 |
|---|---|---|---|---|---|---|
| phase | N* | H | H | H | H | H |
| $a$, Å | | 33.87 | 31.13 | 30.16 | 28.72 | 26.00 |
| low angle | | | | $S$, $10^{-3}$ Å$^{-1}$ | | |
| | | cal obs | cal obs | cal obs | cal obs | cal obs |
| $(h^2 + k^2 - hk)$ | | | | | | |
| 1 | | 34.1 34.0 | 37.1 37.1 | 38.3 38.3 | 40.2 40.3 | 44.4 44.4 |
| 3 | | 59.1 59.1 | 64.2 64.4 | 66.3 66.3 | 69.6 69.6 | 76.9 76.9 |
| 4 | | 68.2 68.4 | 74.2 74.0 | 76.6 76.2 | 80.4 80.2 | 88.8 |
| 7 | | 90.2 90.2 | 98.1 | 101.3 101.6 | 106.4 | 117.5 |
| high angle | | | | $S \pm 0.02$, Å$^{-1}$ | | |
| | $(3.29)^{-1}$ | $(3.32)^{-1}$ | $(3.30)^{-1}$ | $(3.30)^{-1}$ | $(3.30)^{-1}$ | $(3.32)^{-1}$ |

Derivative: **G6**

| $c$, % w/w | 30 | 40 | 50 | 70 | 80 |
|---|---|---|---|---|---|
| phase | N* | H | H | H | H |
| $a$, Å | | 34.79 | 31.75 | 29.87 | 28.56 |
| low angle | | | | $S$, $10^{-1}$ Å$^{-1}$ | |
| | | cal obs | cal obs | cal obs | cal obs |
| $(h^2 + k^2 - hk)$ | | | | | |
| 1 | | 33.2 33.0 | 36.4 36.4 | 38.7 38.6 | 40.4 40.4 |
| 3 | | 57.5 | 63.0 62.7 | 67.0 66.9 | 70.0 70.1 |
| 4 | | 66.4 66.6 | 72.7 72.8 | 77.3 77.6 | 80.9 81.0 |
| 7 | | 87.8 87.8 | 96.2 96.6 | 102.3 102.1 | 107.0 |
| high angle | | | | $S \pm 0.02$, Å$^{-1}$ | |
| | $(3.34)^{-1}$ | $(3.35)^{-1}$ | $(3.34)^{-1}$ | $(3.34)^{-1}$ | $(3.35)^{-1}$ |

[a] $c$ is the concentration; $a$ is the dimension of the two-dimensional hexagonal unit cell; low and high angles refer to the two distinct regions of the diffraction pattern (see text); $S$ (defined in ref 14) is the reciprocal spacing of the reflection with $h.k$ indices; obs refers to the observed spacing, while cal refers to the ones calculated for two-dimensional hexagonal structures with the reported lattice parameters.[16]

detected in the more diluted isotropic solution.

From a structural point of view, these results strongly indicate that **G1**, **G3**, and **G6** behave as the **G2** derivative previously investigated:[5] in the previous paper the liquid–crystalline phases were described to consist of rod-shaped aggregates, each rod being composed of a stacked array of planar tetramers equally spaced at a distance of about 3.3 Å and formed by Hoogsteen-bonded guanosine moieties. These cylinders were identified as the structural units that can form either hexagonal or cholesteric mesophases depending on water content. In the present case, the same structural model can be assumed as it is again effective for explaining the X-ray diffraction data and the optical observations.

Concerning in particular the hexagonal phase, the position of the peaks observed at low angle in all the investigated derivatives appears to change as a function of the water content: this corresponds to the dependence of the hexagonal lattice parameter (which in this case corresponds to the minimum distance between two neighboring objects) on the sample concentration which is shown in Figure 3 at 25 °C (it must be noticed that the unit cell dimension of all derivatives is practically temperature independent in the range from 20 to 40 °C). By using the model of guanosine cylindrical aggregates embedded in a water matrix and making the assumption that water does not penetrate the rods (usual for classical lyotropic hexagonal phases),[17] it is possible to determine the cylinder radii by using the following equation

$$R_{rod} = (\sigma C_v/\pi)^{1/2} \quad (1)$$

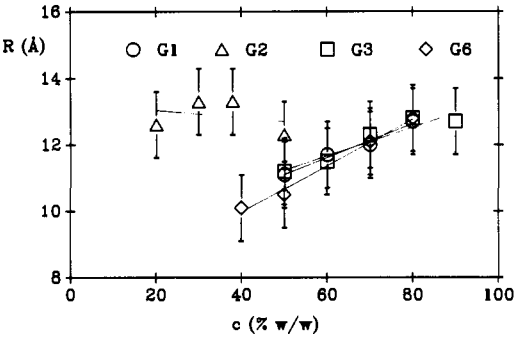


**Figure 4.** Radii of the rod-shaped aggregates in the hexagonal phase at 25 °C as a function of guanosine derivative concentration. The radii are calculated supposing the aggregates to be straight rods of circular section containing only guanosine molecules. The specific volume of water and of all **G1**, **G2**, **G3**, and **G6** derivatives are considered to be 1.000 and 0.651 cm$^3$ g$^{-1}$, respectively. Data for **G2** are taken from ref 5.

where $\sigma$ is the unit cell surface and $C_v$ the volume concentration of the sample. The radii obtained at 25 °C for the rod-shaped aggregates in the case of **G1**, **G3**, and **G6** derivatives, calculated by using the value of 0.651 cm$^3$ g$^{-1}$ as specific volume,[19] are reported in Figure 4 as a function of the water content: it is

(17) Luzzati, V. In *Biological Membranes*; Chapman, D., Ed.; Academic Press: London, 1968: Chapter 3.

(18) *International Tables for X-ray Crystallography*; The Kynoch Press: Birmingham, 1952: Vols. 1 and 2.

(19) Iball, J.; Morgan, C. H.; Wilson, H. R. *Nature (London)* **1963**, *199*, 688–9.

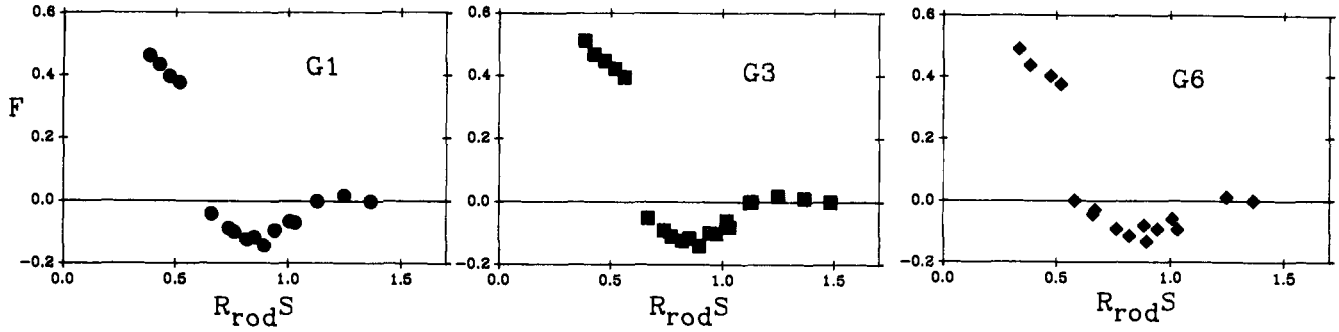


**Figure 5.** Determination of the signs of the structure factors in the hexagonal phase of **G1**, **G3**, and **G6**. The experiments were performed at different water content at 25 °C: the normalized structure factors (see text) are plotted as a function of the product $R_{rod}S$.

interesting to observe that, contrary to what was observed in the case of **G2** derivative,[5] the radii appear to decrease when the water content increases. Even if this variation is of about the same order as the estimated error, the general behavior seems to indicate that the aggregates are not as rigid as **G2** or that they interact in a more specific way with water than was assumed in the model.

To obtain more direct structural information about the hexagonal phase, the analysis of the X-ray diffraction data has been extended also to the intensity of reflections. In particular, the relation between the electron density distribution in the sample and the observed intensities is given in the case of a hexagonal phase by[17]

$$\rho(x,y) = c' \sum F(h,k) \cos 2\pi(hx + ky) \qquad (2)$$

where $\rho(x,y)$ is the two-dimensional electron density distribution, $c'$ a normalizing factor, $F(h,k)$ is the structure factor of the reflection with Miller indices $h,k$, and the sum concerns all $h,k$ peaks observed. As the structure factors are calculated from the diffracted intensities according to

$$|F(h,k)| = [I(h,k)/m(h,k)]^{1/2} \qquad (3)$$

where $I(h,k)$ is the observed intensity of the reflection with $h,k$ indices and $m(h,k)$ is its multiplicity; we do not have any information about the sign of the structure factors. However, the unit cell dependence on the water concentration allows the solution of the crystallographic "phase problem": in fact, by performing the so-called "swelling" experiment, we can reconstruct the continuous structure factor function (the form factor of the rod-shaped aggregate) and then, by considering the position of the inversion points, assign to any structure factor the correct sign.[20]

As usual,[21] the intensities of all reflections observed in any experiment of the three different swelling series (one for each derivative) were normalized so that

$$\sum I(h,k) = \sigma/\sigma_{min} \qquad (4)$$

where $\sigma_{min}$ is the unit cell surface for the sample with the smallest cell dimension in the series. The corresponding structure factors were plotted as a function of the product $R_{rod}S$ and the position of zeros inferred; Figure 5 reports the curves obtained by using the signs derived in this way. It must be noticed that, even if these curves do not exactly represent the continuous structure factor functions, as some possible small changes of the inner structure of the rods cannot be excluded, they appear, however, sufficiently smooth to indicate with reasonable certainty the position of the zeros and to support the correctness of the derived signs.

The electron density distributions corresponding respectively to samples containing 50% of **G1**, **G3**, and **G6** and calculated[22] from the intensity data of Table II are reported in Figure 6: these maps clearly show the electron dense rod section surrounded by a smooth region of lower electron density, which can be easily associated with water. Two interesting features must be underlined, which strongly support our proposed model: first, the rod dimensions, which can be directly measured in the electron density maps, are in excellent agreement with the experimental data (see, for example, Table II); secondly, due to the higher experimental resolution (about 10 Å) with respect to the previous reported data on **G2**,[5] the central region of the rods appears to be characterized

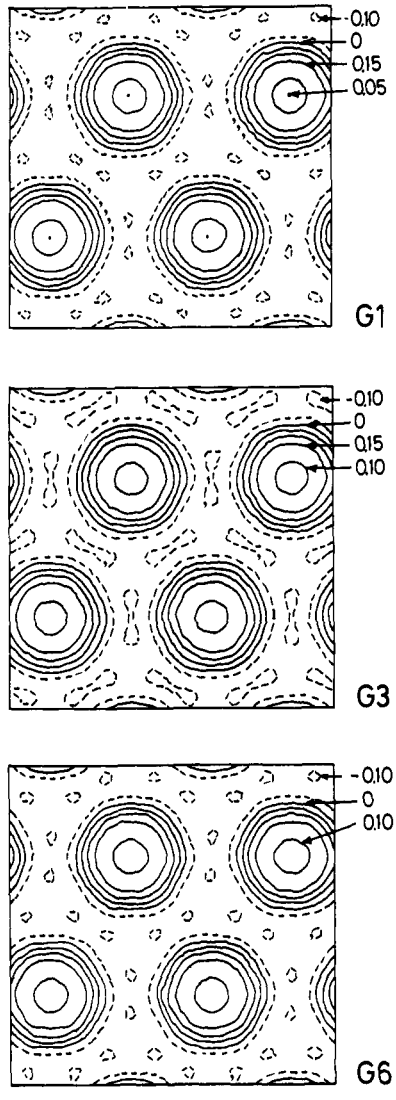


**Figure 6.** Electron density distribution of the hexagonal phase of **G1**, **G3**, and **G6** at $c$ = 50% and $T$ = 25 °C. The observed structure factors (see Table II) are normalized as reported in refs 23 and 24 to give a dimensionless expression of the electron density fluctuation: the density lines are equally stacked, with an increment of 0.5, and negative levels are dotted. As the level of equidensity lines is not self-evident everywhere, the relative value (with respect to zero) is reported on some lines.

(20) Franks, N. P. *J. Mol. Biol.* **1976**, *100*, 345–58.
(21) Blauroch, A. E. *J. Mol. Biol.* **1971**, *56*, 35–52.
(22) The intensity data are normalized such that $\sum I(h,k) = 1$; in this condition, $\rho(x,y)$ becomes a normalized dimensionless expression of the electron density fluctuation (see refs 23 and 24 for more details).

**Table II.** Structure Factors and Radii of the Cylindrical Aggregates of Samples Containing 50% of Guanosine Derivatives at 25 °C[a]

| derivative | G1 | G3 | G6 |
|---|---|---|---|
| *a*, Å | 33.62 | 33.87 | 31.75 |
| $R_{rod}$, Å | 11.09 | 11.17 | 10.47 |
| $R_{map}$, Å | 11.25 | 11.48 | 10.63 |
| **structure factors** | **G1** | **G3** | **G6** |
| *F*(1,0) | +0.390 | +0.392 | +0.391 |
| *F*(2,1) | −0.034 | −0.039 | −0.039 |
| *F*(2,0) | −0.083 | −0.084 | −0.081 |
| *F*(3,1) | −0.055 | −0.046 | −0.053 |

[a] *a* is the unit cell dimension; $R_{rod}$ is the radius of the rod-shaped aggregates calculated by supposing straight rods of circular section containing only guanosine molecules and a specific volume of 1 and 0.651 $cm^3\ g^{-1}$ for water and guanosine derivatives, respectively; $R_{map}$ is the radius of the aggregate measured from the *zero* electron density level in the maps of Figure 6. The structure factors (see text) are obtained from diffracted intensities normalized as reported in refs 23 and 24 such that $\sum I(h,k) = 1$.

by a gradual decrease of the electron density, which can be explained by considering the presence of the hole in the middle of the guanosine tetramer.[25]

In regards to the high angle diffraction peak, it is interesting to observe its behavior when the water content is changed. As already reported,[5] this peak is associated with the distance between the stacked planar tetramers: it is worthwhile noticing that, for a single guanosine derivative, the spacing and the half-height width of this reflection appear to be constant at all investigated concentrations, irrespectively of the sample cholesteric or hexagonal organization (see Table I). However, when different compounds are considered, the corresponding peak spacing appears to be different, going from a mean value of 3.39 ± 0.01 Å for the **G1** derivative to a mean value of 3.34 ± 0.01 Å for the **G6** and to the mean value of 3.31 ± 0.01 Å for the **G3** derivative. These data can be compared with the previously reported 3.32 ± 0.01 Å value relative to the **G2** liquid crystalline phases and will be discussed later.

No additional periodicities corresponding to the length of possible discrete cylindrical oligomers which aggregate head-to-tail to give the final columnar structures could be detected clearly.

**Circular Dichroism Studies.** This spectroscopic technique, due to its sensitivity to stereochemical variations, is ideal for following the process of association from the isolated molecules to the supramolecular aggregate and finally to the formation of the cholesteric phase; furthermore, it allows the determination of the handedness of the cholesteric superhelix.

Figure 7 presents the concentration dependence of the CD spectrum of **G2** which was the subject of our previous X-ray diffraction and microscopic study. The spectrum in the region of the first two absorptions of the guanosine chromophore is negative at low concentration and then becomes positive and reaches, at the maximum concentration compatible with the isotropic solution, a shape not very different from that of the four-stranded helix of poly(G),[26] even though the intensity is considerably smaller. At higher concentration an enormous negative band is observed which is associated with the formation of the cholesteric phase[27] (upper inset in Figure 7). From the sign of this band, the handedness of the cholesteric can be inferred if information on the nature of the objects which compose the

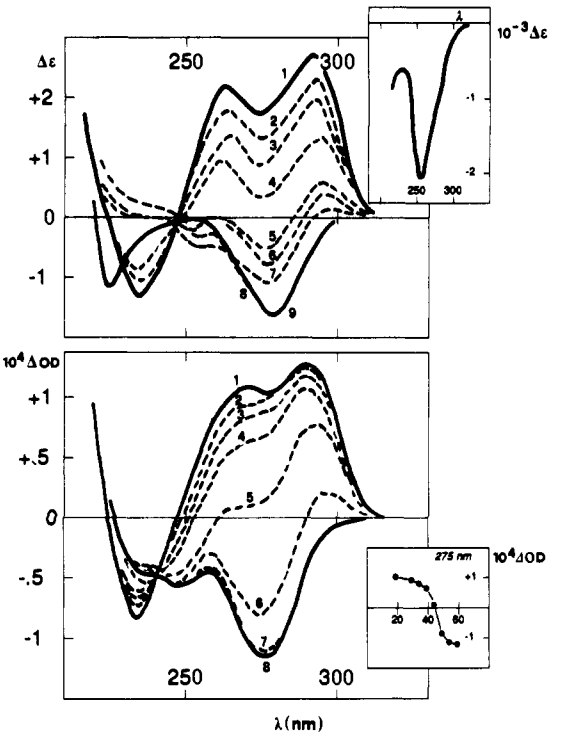


**Figure 7. G2.** Upper part: circular dichroism spectra of aqueous solutions as a function of the concentration, *c* = 2.31% (1), 1.74% (2), 1.56% (3), 1.16% (4), 1.04% (5), 0.87% (6), 0.78% (77), 0.31% (8), and 0.003% (9). In the insert is reported the circular dichroism of a cholesteric solution ($c \approx 2.5\%$) with planar orientation. Lower part: circular dichroism spectrum of a buffered (pH 7) diluted aqueous solution ($c \approx 0.003\%$) as a function of the temperature, *T* = 20 °C (1), 30 °C (2), 35 °C (3), 40 °C (4), 45 °C (5), 50 °C (6), 55 °C (7), 60 °C (8). In the insert is reported the plot of CD at 275 nm vs the temperature.

cholesteric is available. In this case, we already know that these objects consist of chiral cylindrical aggregates composed of a stacked array of planar tetramers formed by Hoogsteen-bonded guanosine moieties. These chiral rods interact to give a cholesteric superhelix. Similarly to DNA double helixes,[28] our objects, which are four-stranded helixes, have negative diamagnetic and optical anisotropy and also negative linear dichroism as the main transitions of the guanine chromophore and in particular those around 255 nm are in-plane polarized.

The handedness of the cholesteric superhelixes (i.e., the sign of the pitch length *p*) can be correlated to their CD spectra by eq 5[29]

$$(OD_L - OD_R)_j = p\nu_j^3 \Delta n (OD_\parallel - OD_\perp)/2(\nu_j^2 - \nu_0^2) \quad (5)$$

where $(OD_L - OD_R)_j$ is the CD at frequency $\nu_j$, $\nu_0$ is the frequency of the selective reflection which is correlated to the cholesteric pitch that we know from the fingerprint texture to be in the IR region, $\Delta n$ is the optical anisotropy, *p* is positive for a right-handed helix, and $(OD_\parallel - OD_\perp)$ is the linear dichroism of the helix-building objects. Therefore in our case, negative CD indicates a left-handed cholesteric. We are very confident in this assignment as we have already studied by CD the handedness of thermotropic,[30] micellar,[31] and DNA[28] cholesterics and in all cases the assignments were confirmed by independent techniques. In particular, for DNA cholesterics, which are strictly related to the present system, our assignment is in agreement with recent independent research.[32]

(23) Luzzati, V.; Mariani, P.; Delacroix, H. *Macromol. Chem. Macromol. Symp.* **1988**, *15*, 1–17.
(24) Mariani, P.; Luzzati, V.; Delacroix, H. *J. Mol. Biol.* **1988**, *204*, 165–89.
(25) This fact is compatible with the presence of the sodium or ammonium ions inside the central hole.[7,10] The estimated volume of the cavity is about 30 $Å^3$ per tetramer and hence the "local" electronic density is about 0.33 $e^-/Å^3$ for both the cations. This value is roughly equal to that of water but considerably smaller than the average value for the guanosine derivatives (0.47 $e^-/Å^3$).
(26) Gottarelli, G.; Palmieri, P.; Spada, G. P. *Gazz. Chim. Ital.* **1990**, *120*, 101–7.
(27) Saeva, F. D. In *Liquid Crystals*; Saeva, F. D., Ed.; Marcel Dekker: New York, 1979.
(28) Spada, G. P.; Brigidi, P.; Gottarelli, G. *J. Chem. Soc., Chem. Commun.* **1988**, 953.
(29) Sakmann, E.; Voss. J. *Chem. Phys. Lett.* **1972**, *14*, 528. Dudley, R. J.; Mason, S. F.; Peacock, R. D. *J. Chem. Soc., Faraday Trans. 2* **1975**, 997.
(30) Gottarelli, G.; Samori. B.; Strammenos, C.; Torre, G. *Tetrahedron* **1981**, *37*, 395.
(31) Spada, G. P.; Gottarelli, G.; Samori, B.; Bustamante, C.; Wells, K. S. *Liq. Cryst.* **1988**, *3*, 101.

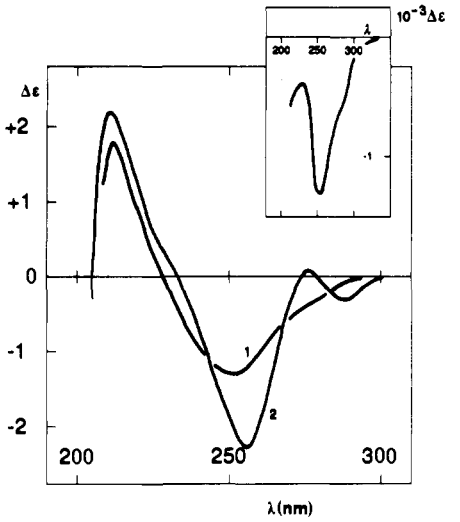


**Figure 8. G1.** Circular dichroism spectra of aqueous solutions at $c$ = 0.007% (1) and $c$ = 3%. In the insert is reported the CD of a cholesteric solution ($c \approx 32\%$) with planar orientation.

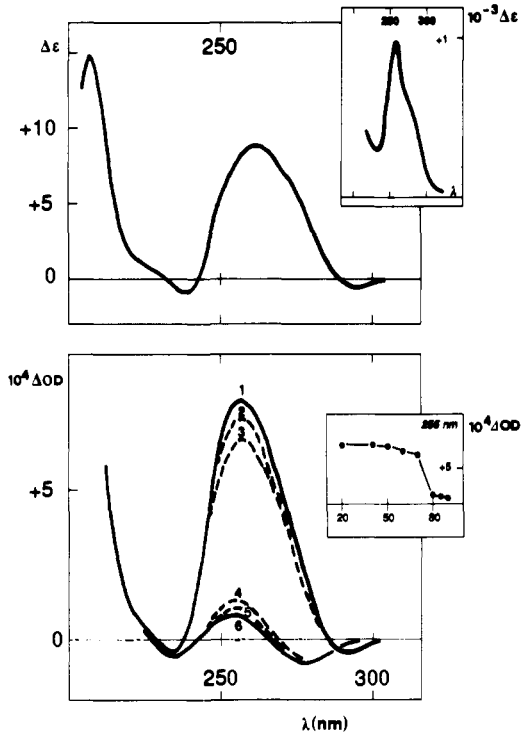


**Figure 9. G3.** Upper part: circular dichroism spectra of buffered (pH 7) aqueous solutions at $c$ = 2.7% and $c$ = 0.003%; the two spectra are superposable. The insert shows the CD of a cholesteric solution ($c \approx 8\%$) with planar orientation. Lower part: CD spectra of a buffered (pH 7) diluted aqueous solution ($c$ = 0.005%) as a function of the temperature; $T$ = 20–40 °C (1), 60 °C (2), 70 °C (3), 80 °C (4), 85 °C (5), 90 °C (6). In the insert is reported the plot of CD at 255 nm vs the temperature.

Aggregation to the four-stranded helix occurs also at higher dilution in phosphate buffer pH 7.0. In Figure 7 (lower part) the dependence of the CD spectrum on the temperature in a buffered solution is reported. The trend is similar to that previously discussed and exhibited by the water solution as a function of the solute concentration and displays the aggregation equilibrium with a "melting temperature" ($T_m$) of about 40–50 °C.

The CD behavior of **G1**, **G3**, **G4**, and **G6** is reported in Figures 8–10. The monomer **G1** shows some variations of the spectrum

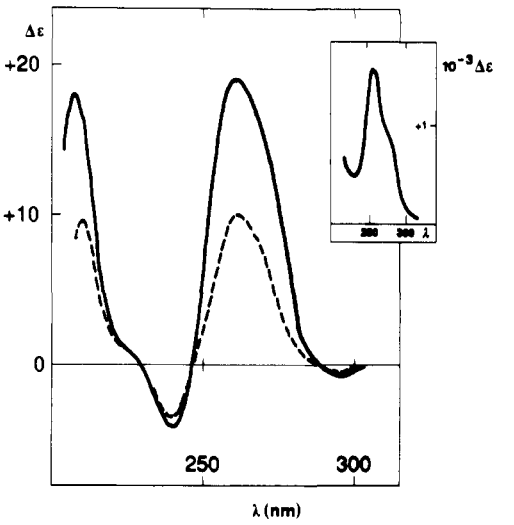


**Figure 10. G4** and **G6**. Full line: circular dichroism spectra of buffered (pH 7) aqueous solutions of **G6** at $c$ = 8.8% and $c$ = 0.003%; the two spectra are superposable. The insert shows the CD of a cholesteric solution ($c \approx 20\%$) with planar orientation. Dashed line: circular dichroism spectra of buffered (pH 7) aqueous solutions of **G4** at $c$ = 6% and $c$ = 0.003%; the two spectra are superposable.

as a function of the concentration in the isotropic phase and then a massive negative CD corresponding to the formation of a left-handed cholesteric. The isotropic spectra of **G3**, **G4**, and **G6** (in phosphate buffer pH 7.0) do not show concentration dependence; this indicates that aggregation (to the four-stranded helix) occurs at high dilutions. In the case of **G3**, also the temperature dependence is reported. This shows that the aggregation occurs below ca. $T$ = 80 °C, while when $T \geq 80$ °C the spectrum is typical for a nonaggregated single strand oligomer.[33] It should be noted that, as expected, the $T_m$ for the trimer is greater than that of the dimer. Furthermore, the CD of the cholesteric phases is positive for derivatives **G3**, **G4**, and **G6**, indicating a right-handed cholesteric.

We have also checked the handedness of the cholesterics by recording the CD spectra of ethidium bromide dissolved in the magnetically aligned cholesterics. Ethidium bromide is known to intercalate in DNA[34] and in our case behaves similarly:[35] its planar structure fits between the tetrameric planes and is perpendicular to the symmetry axes of the aggregates. As its transition at ca. 500 nm is in-plane polarized,[34] its linear dichroism in our rod-like aggregates should be negative. The spectra (see Figure 11 where also the CD of ethidium bromide dissolved in the left-handed cholesteric formed by fragments of DNA[28] is reported as an empirical reference) indicate left-handed cholesterics for **G2** and right-handed cholesterics for **G3** and **G6**. For **G1** we could not observe significant CD signals in the dye absorption region; this seems to indicate that in this case no intercalation takes place. In order to have information about the structure of the chiral aggregates which are formed in isotropic solutions and then correlate to form liquid crystals, one needs a model to calculate the CD spectra of the possible candidates. To check the model one also needs a known structure which is reasonably similar to the ones under investigation.

It is known that polyguanylic (poly(G)) and polydeoxyguanylic (poly(dG)) acids in solution form stable four-stranded helixes. The structure of these helixes is known from fiber X-ray studies[36] and is very similar to that of our chiral cylindrical aggregates.

(32) Livolant, F.; Maestre, M. F. *Biochemistry* **1988**, *27*, 3056 and references therein.

(33) Gray, D. M.; Bollum, F. J. *Biopolymers* **1974**, *13*, 2087–102.

(34) Ohmes, E.; Pauluhn, J.; Weidner, J.-U.; Zimmermann, H. W. *Ber. Bunsenges. Phys. Chem.* **1980**, *84*, 23–6. Zimmermann, H. W. *Angew. Chem., Int. Ed. Engl.* **1986**, *25*, 115–30.

(35) Bouhoutsos-Brown, E.; Marshall, C. L.; Pinnavaia, T. J. *J. Am. Chem. Soc.* **1982**, *104*, 6576–84.

(36) Arnott, S.; Chandrasekaran, R.; Marttila, C. A. *Biochem. J.* **1974**, *141*, 537. Zimmermann, S. B.; Cohen, G. H.; Davies, D. R. *J. Mol. Biol.* **1975**, *92*, 181.

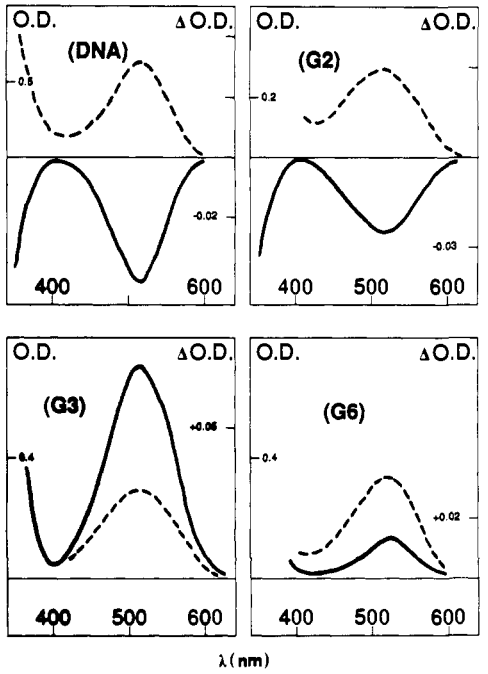


**Figure 11.** The absorption (broken lines) and the induced circular dichroism (full lines) spectra of the ethidium bromide dissolved in cholesteric solutions of **G2**, **G3**, and **G6** with planar orientation (with DNA as a reference).

The four-stranded helix of poly(G) is right-handed and its detailed geometry is fairly well described.

The chromophoric part of the poly(G) four-folded helix is constituted by a stacked array of planar guanosine tetramers (just like our aggregates). Each tetrameric plane is rotated clockwise with respect to the preceding one of ca. 30°.

CD calculations were successfully carried out with the exciton model for the poly(G) four-folded helix.[26] They are therefore useful for solving the problem of the handedness of our aggregates in solution.

Basically, for a right-handed structure composed of planar tetramers, two positive couplets are expected and the high-energy one dominates. The introduction of small out-of-plane distortions in the tetramer seems to modify only the sign of the low-energy band.[37] For diagnostic purposes, the handedness of the aggregate can be deduced by the sign of the couplet at ca. 250 nm; briefly, a positive exciton couplet is correlated to a right-handed helix, a negative couplet to a left-handed helix.

For **G2** the isotropic spectrum at maximum concentration is similar to that of the four-stranded helix of poly(G) and poly(dG),[38] although its intensity is considerably smaller; the couplet at around 250 nm is positive, and we can infer also that **G2** aggregates are right-handed. For **G1** the spectrum shows a quasi-mirror image sequence of the bands and could indicate a left-handed helical structure. For **G3**, **G4**, and **G6** the spectra are more complex, but the diagnostic couplet is positive, indicating a right-handed structure.[39]

## Discussion

As reported for **G2** in a previous paper,[5] the building structure of all the mesophases is a chiral rod-shaped aggregate composed of a stack of Hoogsteen-bonded guanine tetramers. At high dilution, these aggregates give rise to isotropic solutions which, at higher concentration, become cholesteric mesophases characterized by a weak correlation between the rods. By further increasing the concentration, hexagonal mesophases are obtained in which the rods are arranged in a highly ordered array.

In the case of **G1**, only hydrogen bonds and stacking forces are active in keeping together the tetramers to form the columnar aggregate. For **G2**, **G3**, **G4** and **G6** the macrostructure is held together also by phosphodiester bridges.

The finding that the periodicity along the rod axis is slightly greater for **G1** (3.4 Å) than for the other derivatives (3.3 Å) is likely to reflect the fact that this molecule is the only one with a free end phosphate.

Other instructive information is obtained from the critical concentration at which the cholesteric phases appear. For the homologous series **G2**, **G3**, **G4**, and **G6** this concentration reflects a balance between hydrophilic and hydrophobic groups: **G2**, in which this ratio is the lowest, originates the cholesteric phase at higher dilution, while **G6**, in which this ratio is the highest, gives rise to the cholesteric phase only at high concentration. Monomeric derivatives instead do not follow this trend: their ability to form mesophases is related to the position of the phosphate group and probably to its capacity to substitute phosphodiester bridges in connecting different monomers.

It is also interesting to notice the effect of dilution on the lattice parameter of the hexagonal phases. While the behavior of **G1**, **G3**, and **G6** are similar, showing a moderate dependence of the intercolumnar distance on the concentration, in the case of **G2** this dependence is dramatic. This trend is confirmed in a completely independent way for the cholesteric phases from measurements of the pitch dependence on the concentration. In general one expects an increase of the pitch with dilution as the distance between the rods increases and their chiral interactions decrease. Again the concentration dependence for **G2** is much more pronounced than for the other derivatives (including **G4**).

These anomalous dependences of **G2** are likely to be related to its more pronounced hydrophobic character: its rod-shaped aggregate interacts to a lesser extent with water, which acts merely as a diluting solvent, while, for other derivatives, specific interactions seem to be operative.

**Handedness of the Cholesteric Mesophases.** While **G1** and **G2** give rise to a left-handed cholesteric, **G3**, **G4**, and **G6** give the opposite handed phases. These data seem at first glance rather erratic; however, it is possible to give a tentative explanation based on the pitch values and on the intensity of the CD spectra of the aggregates in isotropic solution. We should first assume that the characteristics of the cholesterics and in particular their handedness are connected to the stereochemistry of the chiral columnar aggregates. In addition to Hoogsteen H-bonds, each individual column is kept together by two general types of forces: phosphodiester bridges and noncovalent interactions. The former forces are dominant in **G6**, while the latter are the exclusive ones for **G1**. The handedness of the four-stranded helix imposed by the two forces is not necessarily the same. On the basis of CD measurements in isotropic solution, for **G1** the noncovalent interactions seem to generate a left-handed 4-fold helix, while for **G6** the covalent forces generate a right-handed structure (see the right-handed 4-fold helix of poly(G)).[26] It therefore seems straightforward that the two cholesterics have opposite handedness. For **G2**, **G3**, and **G4** both forces must be operative. For **G2** the nonbonded forces seem to give a strong contribution to the overall chirality of the rod (its CD spectrum which reflects only the chromophoric interactions and is not strictly connected to the overall external shape of the aggregate shows a trend indicative of a right-handed 4-fold helix but with intensity much weaker than for **G6**) and give rise to a left-handed cholesteric as for **G1**.[40]

(37) Cech, C. L.; Tinoco, I., Jr. *Nucl. Acid Res.* **1976**, *3*, 399–404.
(38) Howard, F. B.; Frazier, J.; Todd Miles, H. *Biopolymers* **1977**, *16*, 791. Williams, A. L., Jr.; Moore, D. S. *Biopolymers* **1983**, *22*, 755 and references therein.
(39) The spectra display a situation similar to that reported by Cech and Tinoco[37] for the four-stranded right-handed helix of poly(I) (in which I was assumed to possess spectral properties very similar to G). In this paper it is emphasized that the first negative low energy band is not indicative of a left-handed helix.
(40) More precisely, while for **G2**, **G3**, **G4**, and **G6** the noncovalent forces are of the same type for each discrete aggregate shown in Figure 12 and must give identical negative contributions to the overall chirality of the columnar aggregates, in the case of **G1**, due to the presence of the free phosphate group, the noncovalent forces are different from the other cases. The fact that these forces give also in this case a left-handed contribution to the chirality of the aggregate is fortuitous but does not invalidate the model proposed.

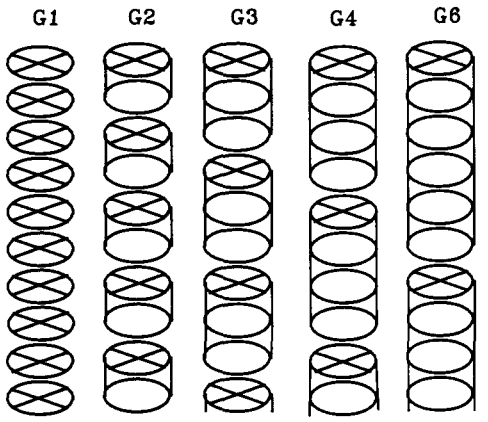


**Figure 12.** A sketch of the rod structure for the different compounds according to the model based on the piling up of discrete aggregates. Each circle (in perspective view) represents a Hoogsteen-bonded tetrameric plane. For simplicity the helical distribution along the rod axis is omitted.

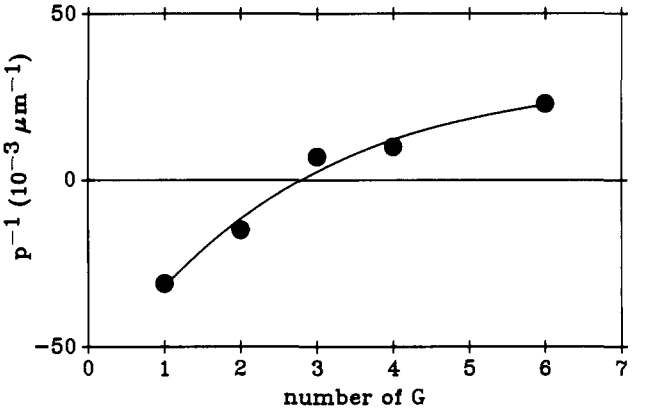


**Figure 13.** Reciprocal pitches ($p^{-1}$) of the cholesterics obtained from compounds **G1**, **G2**, **G3**, **G4**, and **G6**. Data are referred at $(c - c_0) = 0$ and are obtained by extrapolation from plots of $p^{-1}$ vs $c$. The signs − and + refer to left-handed (M) and right-handed (P) cholesterics, respectively.

For **G3** and **G4** the situation is instead similar to **G6**, although the CD spectrum is less intense (but more intense than for **G2**): the noncovalent interactions are probably still important. A support to this explanation is given by the pitch values. As already seen, the concentration at which transition between the isotropic and the cholesteric phases occurs ($c_0$) is different for different compounds. In order to obtain data which can be comparable, the pitches are referred to the same "reduced" concentration ($c - c_0$), which was chosen at the highest possible dilution ($c = c_0$). These data are reported together with the sense of cholesteric in Figure 12.

As expected, the homochiral 4-folded helices of **G1** and **G6** form the most compact cholesteric helices, while **G2**, **G3**, and **G4**, for which two opposite chiralities seem to coexist, give less compact cholesterics.

These findings give some indication toward the answer to the problem posed in our previous paper: do the individual molecules of **G2**, **G3**, **G4**, and **G6** self-aggregate to give discrete four-stranded aggregates (composed of 8, 12, 16, and 24 guanines, respectively, which further pile up to give a fully developed helix) or do they form continuous structures?

The simple explanation offered above for justifying the variation of the cholesteric handedness for different compounds indicates a discrete model. Recent and preliminary small angle neutron scattering data obtained in diluted solution indicate also the presence of discrete aggregates.[41]

## Experimental Section

**Synthesis.** The fully protected oligodeoxyguanylates were obtained by a modified phosphotriester method,[42] with the following overall yields: dimer 77%, trimer 65%, tetramer 52%, and hexamer 41%. After deprotection the crude products were purified up to an HPLC titer ≥95% by column chromatography. The dimer was obtained in 70% yield with Lichroprep RP18 as the stationary phase. The longer oligomers could be obtained, albeit in low yield, only after several elutions from silanized silica gel. With Lichroprep RP18 or DEAE-Sephacel almost all the material remained irreversibly adsorbed by the sorbent. This behavior of guanylate-rich oligonucleotides has already been reported.[43]

**X-ray Diffraction.** X-ray measurements were performed with a conventional generator equipped with a Guinier camera operating in vacuum: a bent quartz crystal monochromator was used to select the Cu K$\alpha$1 radiation. The samples, prepared at the required concentration and left for at least 1 day at room temperature to avoid dishomogeneity, were held between two mica windows in a vacuum-tight cylindrical cell, which, in order to reduce spottiness arising from eventual macroscopic monodomains, was rotated continuously during the exposure. The temperature was controlled by using a circulation thermostat with an accuracy of ±0.5 °C. The diffraction patterns were recorded on a stack of four Kodak DEF-392 films: densitometric traces were obtained by using a Joyce–Loebl Mk IIIb microdensitometer, and the relative intensities of the reflections were calculated as reported in ref 44. The electron density of water was assumed to be 0.33 e$^-$/Å$^3$ and that of **G1**, **G2**, and **G6** to be always 0.47 e$^-$/Å$^3$. X-ray diffraction experiments were also made with a rotating anode generator Rigaku Denki RV 300 equipped with powder diffractometer: Ni-filtered Cu K$\alpha$ radiation (average wavelength 1.54 Å) was used in this case.

**Optical Microscopy.** Microscopic observation were performed with a Zeiss polarizing microscope equipped with a photocamera and a micrometric graduation in the ocular. Preliminary observations were done on peripheral evaporation samples. Cholesteric solutions were inserted into rectangular capillaries (thickness 0.3 mm) sealed with wax; the samples were oriented by putting them in a 5 kG magnet for about 3 h and the texture was observed between crossed polars. From the "fingerprint" oriented samples the pitches were determined by measuring the separation between two lines of equal extinction.

**Circular Dichroism.** CD spectra were recorded with a Jasco J500A spectropolarimeter equipped with a DP100 data processor and with a thermostatted water jacket cell holder. Solutions were prepared by dissolving the compounds in water or in a commercial phosphate buffer (pH 7.0, Merck code 9439) and allowed to stand refrigerated for a week before recording spectra. The induced CD of the cholesteric phases was measured in 10 μm, 100 μm, or 0.1 cm path length cells depending on the concentration of guanine derivatives or dye (concentrations are expressed in % w/w). The planar orientation of the cholesterics was obtained by means of a magnetic field applied perpendicularly to the cell walls or simply (in the case of 10 and 100 μm path length cells) utilizing the surface effect of the cell walls. The alignment was checked by polarizing microscopy.

**Acknowledgment.** We thank CNR and MURST (Italy) for financial support and a referee for stimulating criticism.

**Registry No. G1**, 902-04-5; **G2**, 15180-30-0; **G3**, 32359-57-2; **G4**, 32327-38-1; **G6**, 58626-19-0.

(41) Mariani. P. Unpublished results.
(42) Marugg, J. E.; Tromp, M.; Jhurani, P.; Hoyng, C. F.; van der Marel, G. A.; van Boom, J. H. *Tetrahedron* **1984**, *40*, 73.
(43) Schott, H.; Semmler. R.; Eckstein, H. *J. Chromatogr.* **1987**, *389*, 165–176.
(44) Tardieu. A. Ph. D. Thesis, Universitè Paris-Sud, 1972.